St. Joseph's Journal of Humanities and Science (Volume 2 Issue 2 August 2015) 53-67

St. Joseph's Journal of Humanities and Science
ISSN: 2347 - 5331
http://sjctnc.edu.in/6107-2/

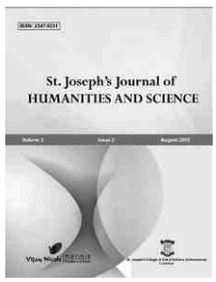

CONFORMATIONAL STABILITY, MOLECULAR STRUCTURE, VIBRATIONAL SPECTRA AND NBO ANALYSIS OF 2,5- DIMETHYLBENZOIC ACID BY DFT METHOD.

- S. Sebastian[a*]
- S. Xavier[a]
- S. Sylvestre[b]
- M. Sathish[c]

Abstract

In this work we analyzed the vibrational (FT-IR and FT-Raman) spectra of 2,5-dimethylbenzoic acid (2,5DMBA) molecule. The total energy of all four possible conformers can be calculated by using Density Functional Theory method with 6-31G(d,p) as basis set. Computational result identify the most stable conformer of 2,5DMBA is C2. The molecular geometry, second order perturbation energies and electron density (ED) transfer from filled lone pairs of Lewis base to unifilled Lewis acid sites for 2,5DMBA molecular analyzed on the basis of Natural Bond Orbital (NBO) analysis. The formation of inter and intramolecuar hydrogen bonding between -OH and -COOH group gave the evidence for the formation of dimer formation for 2,5DMBA molecule. The Molecular Electrostatic Potential (MEP) analysis shows that the negative electrostatic region is over the COOH group and positive electrostatic potential region are present in the ring and all hydrogen. Finally the calculations results were applied to stimulated Infrared and Raman spectra of the title compound.

Keywords: Vibrational spectra; Conformational stability; NBO; MEP; 2,5-dimethylbenzoic acid

INTRODUCTION

Benzoic acid occurs widely in plants and animal tissues along with vitamin B-complex and it is used to raise the salicylate level in blood. It is used in miticides, contrast media in urology, cholocystographic examinations and in manufacture of pharmaceuticals. [1].Recently theoretical study on molecular structure and vibrational analysis of 2,4,5-trimehtybenzoic acid by using FT-IR, FT-Raman and UV techniques by M.Karaback et al [2]. The FT-IR, FT-Raman, NMR, UV and quantum chemical studies on monomeric and dimeric conformations of 3,5-dimethyl-4-methoxybenzoic carried out by M.Karaback et. al [3]. N.Balamurugan et al. [4] analyzed the molecular structure, vibrational spectra, first order hyper polarizability, NBO and HOMO–LUMO analysis of 2-amino-5-bromo-benzoic acid methyl ester. Vibrational spectroscopy is used extensively in organic chemistry, for the identification of functional groups of organic compounds, for studies on molecular conformation, reaction kinetics, etc [5]. Up to our knowledge, the

[a]P.G. & Research Department of Physics, St.Josepch's College of Arts & Science, Manjakuppam, Cuddalore, Tamilnadu – 605107, India.
[b]Department of Chemistry, DMI-St. Eugene University, Chipata 511 026, Zambia.
[c]Research Scholar, Manonmaniam Sundaranar University (MSU), Tirunelveli, Tamil Nadu - 627012, India.
E-mail: sebastian_astro@yahoo.com, Mobile: +91 98436 93193.

vibrational spectra and the theoretical calculations of 2,5DMBA have no reports except our work. FT-IR, NIR-FT-Raman spectroscopy combined with quantum chemical computations has been recently used as an effective tool in the vibrational analysis of drug molecules [6], biological compounds [7] and natural products [8], since fluorescence-free Raman spectra and the computed results can help unambiguous identification of vibrational modes as well as the bonding and structural features of complex organic molecular systems. Both IR and Raman spectroscopy, hyperpolarizability along with HOMO, LUMO analysis have been used to elucidate the information regarding charge transfer within the molecule.

COMPUTATIONAL DETAILS

The requirements of both accuracy and computing economy, theoretical methods and basis sets should be considered. Density functional theory (DFT) has been proved to be useful in treating electronic structure of molecules. The basis set 6-31G(d,p) was used as an effective and economical level of basis set to study fairly large organic molecules. Basing on the points, the density functional three-parameter hybrid model (DFT/B3LYP) at the 6-31G(d,p) basis set was adopted to calculate the properties of the studied molecule in the present work. All the calculations were performed using Gaussian 09W program package [9] with the default convergence criteria without any constraint on the geometry [10]. The optimized structural parameters were used in the vibrational frequency calculations at DFT levels to characterize all stationary points as minima. The assignments of the calculated wavenumbers is assigned by the animation option of Gauss View 3.0 graphical interface for Gaussian programs, which gives a visual presentation of the shape of the vibrational modes [11].

Prediction of Raman Intensities

The Raman activities (S_i) calculated by Gaussian 09 program [09] converted to relative Raman intensities (I_i) using the following relationship derived from the intensity theory of Raman scattering [12, 13].

$$I_i = \frac{f(\nu_0 - \nu_i)^4 S_i}{\nu_i\left[1-\exp\left(-hc\nu_i / kt\right)\right]}$$

Where ν_o is the exciting wavenumber in cm^{-1}, ν_i the vibrational wavenumber of the i^{th} normal mode, *h, c* and *k* are fundamental constants, and *f* is a suitably chosen common normalization factor for all peak intensities. For simulation, the calculated FT-Raman spectra has been plotted using pure Lorentizian band shape with a bandwidth (FWHM) of 10 cm^{-1} as shown in Figure 1 along with theoretical FT-IR spectra.

RESULTS AND DISCUSSION

Molecular Geometry

In our present study has become a greater interest due to three substituents in the ring system namely carboxyl (-COOH) and two methyl group (CH_3) groups. The molecule under investigation has four different conformations. So we calculate the most stable conformer by finding lowest energy in which we found that C2 (E = -499.47393723 a.u) is most stable conformer among others C1 (E = -499.47248430 a.u.), C3(E = -499.46185726a.u.) and C4(E = -499.46378378 a.u.). The computed geometric parameters (bond length and bond angles) for the most stable C2 conformer of 2,5DMBA molecule were computed by B3LYP/6-31G(d,p) method as shown in Table 1. The stable conformer structure contain intramolecular (O….H) bonding between the hydroxyl group and O=COH group. The least stable conformer is obtained for C3 (E = -499.46185726 a.u) as shown in Figure 2. Having gone through the literature survey there is no XRD data is available for 2,5 DMBA molecule so far. The intermolecular interaction is formed by –COOH group of 2,5 DMBA molecule forms a dimer and intramolecular interaction O-H…..O connecting the adjacent dimmers leading to infinite chain in random directions.

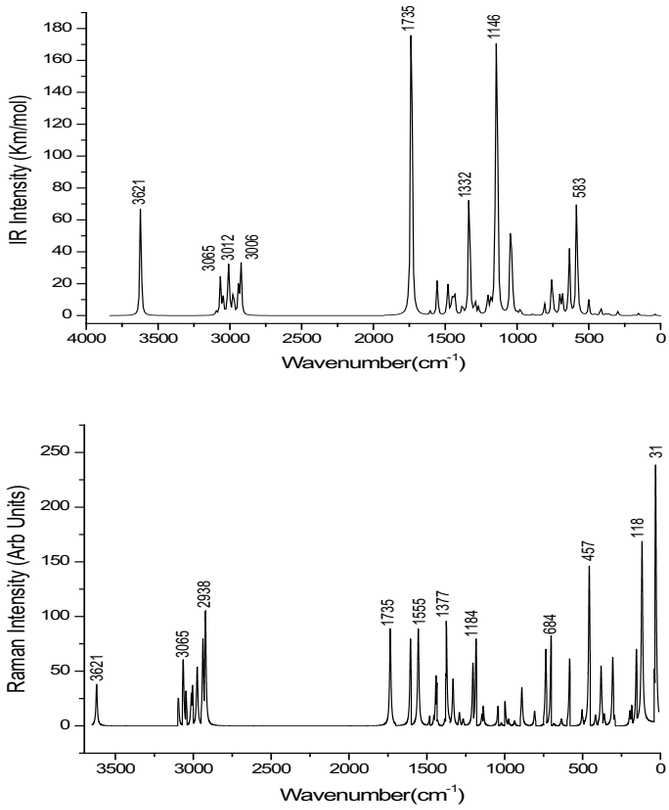

Fig.1 Theoretical Constructed Spectra of FT-IR (Top) and FT-Raman (Bottom) of 2,5DMBA

The changes in bond length of the C-H bond on substituent due to change in charge distribution on the carbon atom of the benzene ring [14, 15] are reported earlier. The carbon atoms are bonded to hydrogen atom with σ bond. The substituent (CH_3 group) for hydrogen can increase electron density at the ring carbon atom as the result decrease in C-H force constant increase in bond length. The computed geometric parameters shows C-H bond length falls in the range C3-H7 = 1.087Å, C4-H8 = 1.088Å, C6-H9 = 1.084 by B3LYP/6-31G(d,p) method. When compared with reported values [2, 3] some deviation can be noted. The deviation may be due to the fact that, low scattering factor of hydrogen atoms involved in the X-ray diffraction experiment. The strong hydrogen bond type of interaction between O20–H21···O40 and O41–H42···O19 is calculated, the distance between O20···O40 and O41···O19 is about both 2.632 Å respectively, are well within the range <3.0 Å for hydrogen interaction [16-18]. The other parameters i.e. the bond angles between the hydrogen bonding are also shown in Table 1. According to international crystallography table [19], the C=O and C-O bond length in the aromatic carboxylic group confirm to an average value of 1.2260 Å and 1.3050 Å respectively. In our present study the C18=O19 and C18-O20 bond length is correlated with above reference values as 1.238 Å and 1.323 Å for dimer by B3LYP/6-31G(d,p) method as shown in Table 2. The C-C bond length for the ring is found to be 1.391 – 1.415 Å by B3LYP/6-31G(d,p) method as well correlate with related molecule [17]. The carbon atom C18 attached to C1 makes bond length C1-C18 which is longer than normal C-C bond. Based on the above comparison although there are some difference between the theoretically computed values and the literature values, the optimized structural parameters can reproduce well the experimental once and they are the basis for the subsequent discussion.

E =-499.47248430 (a.u)

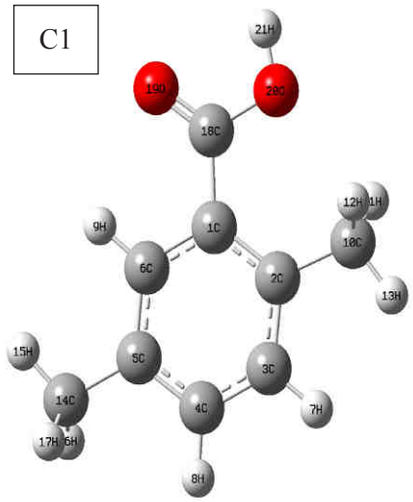

E = -499.47393723 (a.u)

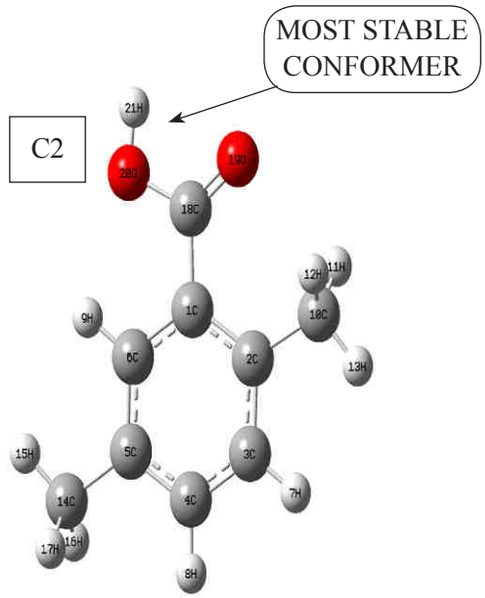

E = -499.46185726 (a.u) **E = -499.46378378 (a.u)**

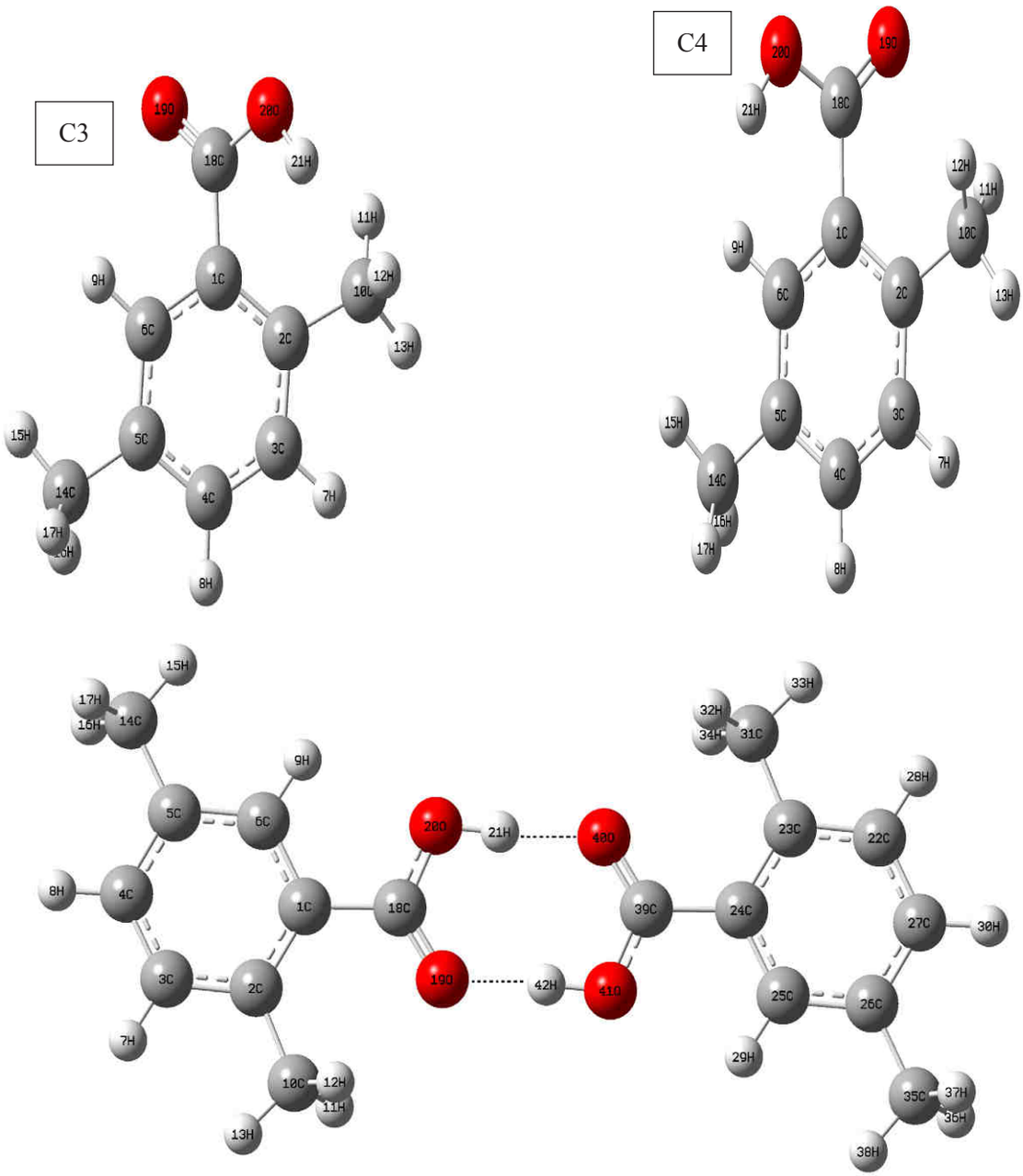

Fig. 2 Molecular Structure and Different Conformation of 2,5DMBA Molecule with Dimer

Table 1. Geometrical Parameters Optimized in 2,5DMBA [bond length (Å) and bond angle (Å) and Dihedral angle (Å)]

Parameters	B3LYP/6-31G(d,p)				
Bond length (Å)	Monomer	Dimer	Bond angle (°)	Monomer	Dimer
C1-C2	1.415	1.415	C4-C3-H7	119.239	119.186
C1-C6	1.406	1.406	C3-C4-C5	120.982	120.951
C1-C18	1.487	1.488	C3-C4-H8	119.378	119.378
C2-C3	1.402	1.402	C5-C4-H8	119.640	119.671
C2-C10	1.509	1.510	C4-C5-C6	117.454	117.417

C3-C4	1.391	1.391	C4-C5-C14	121.094	121.118
C3-H7	1.087	1.087	C6-C5-C14	121.453	121.465
C4-C5	1.401	1.401	C1-C6-C5	122.106	122.209
C4-H8	1.088	1.088	C1-C6-H9	118.449	118.160
C5-C6	1.393	1.393	C5-C6-H9	119.445	119.632
C5-C14	1.510	1.510	C2-C10-H11	111.621	111.674
C6-H9	1.084	1.084	C2-C10-H12	111.621	111.674
C10-H11	1.093	1.093	C2-C10-H13	110.013	109.960
C10-H12	1.093	1.093	H11-C10-H12	105.740	105.874
C10-H13	1.094	1.094	H11-C10-H13	108.854	108.759
C14-H15	1.093	1.093	H12-C10-H13	108.853	108.759
C14-H16	1.096	1.096	C5-C14-H15	111.339	111.324
C14-H17	1.096	1.096	C5-C14-H16	111.364	111.360
C18-O19	1.218	1.238	C5-C14-H17	111.364	111.358
C18-O20	1.362	1.323	H15-C14-H16	107.760	107.774
O20-H21	0.971	1.006	H15-C14-H17	107.759	107.770
Bond angle (°)			H16-C14-H17	107.049	107.049
C2-C1-C6	120.223	120.153	C1-C18-O19	126.257	123.017
C2-C1-C18	120.795	121.785	C1-C18-O20	113.115	114.440
C6-C1-C18	118.981	118.062	O19-C18-O20	120.628	122.543
C1-C2-C3	117.039	116.994	C18-O20-H21	105.082	125.051
C1-C2-C10	124.011	124.374			
C3-C2-C10	118.949	118.631			
C2-C3-C4	122.196	122.277			
C2-C3-H7	118.565	118.537			

Table 2 Intermolecular hydrogen bonding parameters based on B3LYP/6-31G(d,p) method

O20-H21….O40	O20—H21	H21···O40	O20….O40	O20-H21….O40
	1.0062	1.627	2.632	177.74°
O41—H42….O19	O41—H42	H42…..O19	O41…..O19	O41—H42….O19
	1.0062	1.627	2.632	177.74°

Natural Atomic Charge

The natural charge distribution of 2,5DMBA molecule has important influence on the vibrational spectra. It has been recognized that the total charge in molecule/ionic species is a very important parameter on the basis of several important properties. It includes hydrogen bond proton acceptor ability [20], basicity, character (dipole vs zwitterionic) of studied species [21]. The analysis is based on the theory of natural population analysis. Natural atomic charge distribution of 2,5DMBA as shown in Figure 3. The natural atomic charge analysis shows that the substituent of the hydrogen by CH_3 group in 2,5DMBA cause drastic charge distribution in the entire ring systems as evidenced from C2(-0.100e) and C5(-0.235e) for benzoic acid whereas C2(0.021e) and C5(-0.04e) for 2,5DMBA molecule. This shows that CH_3 group exhibits a donating group which donate electron to the ring system.

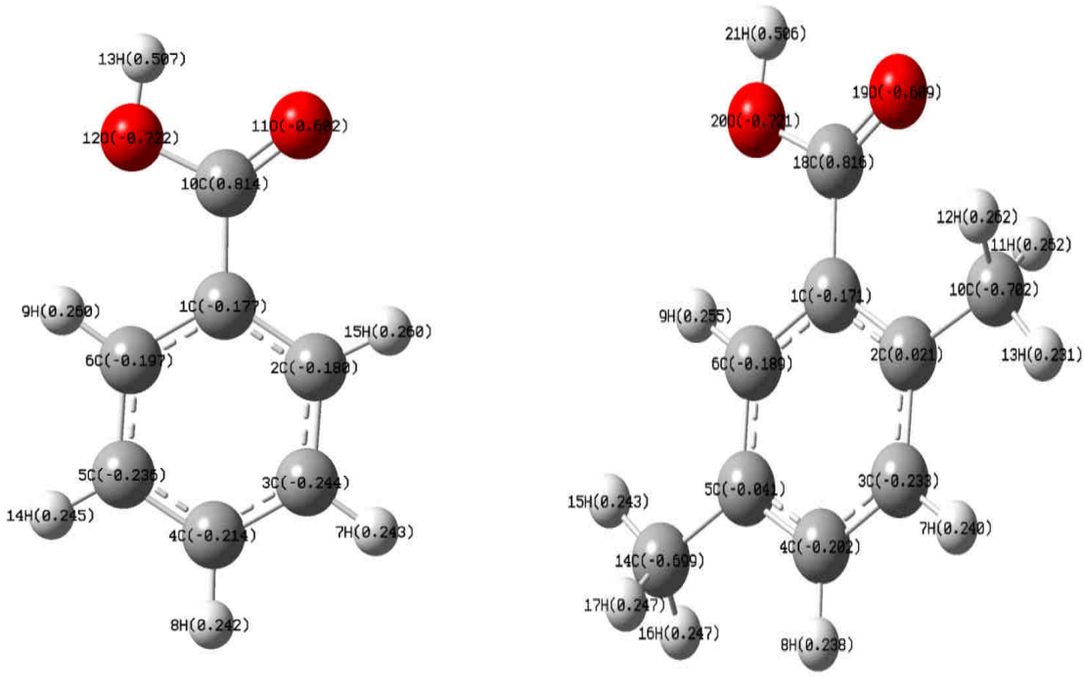

Fig.3 Natural Atomic Charge for Benzoicacid and 2,5DMBA by B3LYP/6-311G(d,p) Method

Potential Energy Surface (PES) Study

The Potential Energy Surface (PES) scan is performed for O-H bond using B3LYP/6-31G(d,p) method for the 2,5DMBA is shown in Figure 4. The dihedral C1-C18-O20-H21 is the relevant coordinate for conformation flexibility within the molecule. During the calculations all the geometrical parameters were simultaneously relaxed while C1-C18-O20-H21 torsional angle were varies in step of 10°, 20°, 30° …360°. For the rotation of the dihedral angle one minimum energy are obtained at 180° it clearly shows that, the O-H in the 180° will give the minimum energy or in other words the O-H group in the angle shows the stable position; it is also evident from the conformational analysis (Refer C2 conformer in Figure 2)

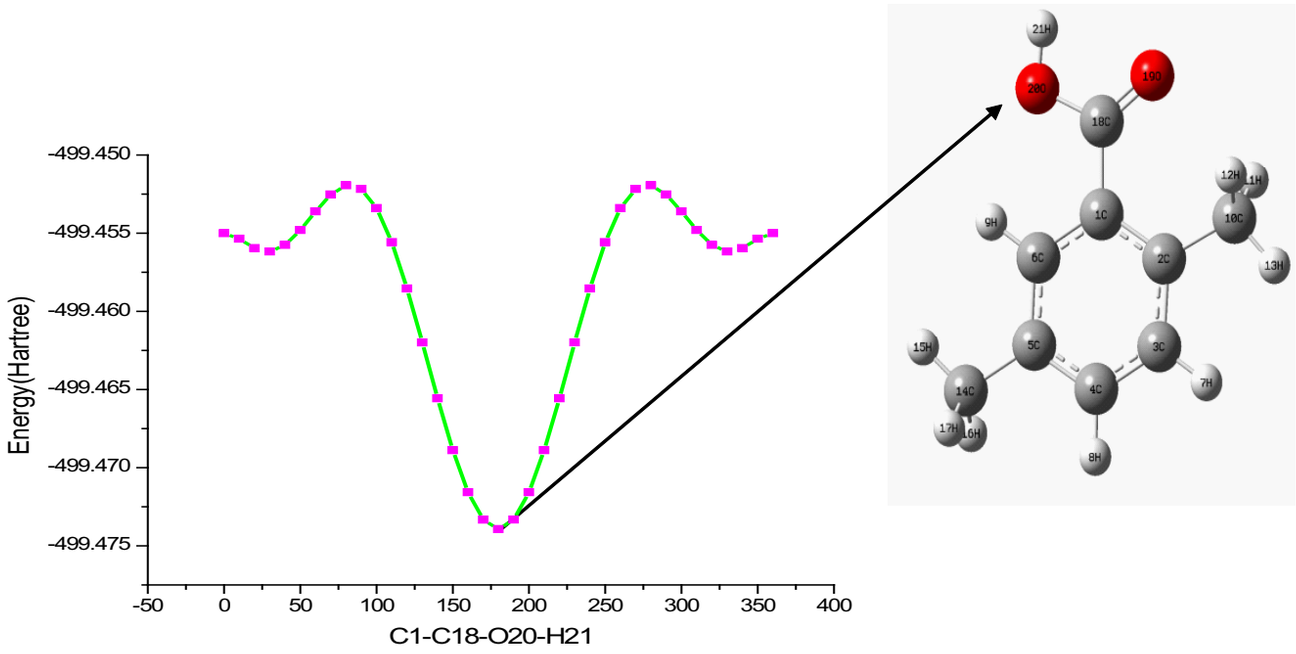

Fig. 4 PES Scan for Dihedral Angle C8-C9-O20-H21 by B3LYP/6-311G(d,p) Method

Natural Bond Orbital Analysis

Natural bond orbital (NBO) analysis provide an efficient method for analyzing intra and intermolecular bonding and interaction among bond and also act as a convenient basis for investigation charge transfer or conjugative interaction in molecular systems [22]. The NBO theory also the assignment of the hybridization of atomic lone pair and of the atoms involved in bond orbitals. Some electron donor orbital, acceptor orbital and in the interaction stabilization energy resulted from the second order micro disturbance theory are reported [23, 24]. The second order fock matrix is used to evaluate the donor-acceptor interactions in NBO analysis [25]. The results of interactions are the loss of occupancy from the localized NBO of idealized Lewis structure into an empty non –Lewis orbital. For each donor (i) and acceptor (j) the stabilization energy E(2) associated with the delocalization i→j is estimated as

$$E^{(2)} = E_{ij} = qiF(i,j)^2 /(\xi_j - \xi_i)$$

Where qi is the donor orbital occupancy, $\xi_i and \xi_j$ are the diagonal element and F(i,j) is the off diagonal NBO fock matrix element. The second order perturbation theory analysis of fock matrix in NBO shows strong intermolecular hyperconjugative interactions, which is shown in Table 3. The larger the value of $E^{(2)}$, the more intensive is the interaction between donor and acceptor and the greater the extent of conjugation of the whole system [26]. The strong intramolecule hyperconjugation interaction of the σ and π electron of carboxylic acid group leads to the stabilization of some part of the ring as evident from the Table 3. The intramolecular interaction is formed by the orbital overlap between C-C, C-H, C=O, C-O to anti bond C-C, C-H, C=O, C-O bond which results Intramolecular Charge Transfer (ICT) causing stabilization of the system. These interactions denote the increase in Electron Density (ED) in C-C, C-H, C=O and C-O bond orbital that weakens the respective bonds. The electron density of the two conjugated single as well as double bond of 2,5DMBA is (~1.9e) which shows the strong delocalization occuring in the molecule. The most strong intramolecule hyperconjugative of σ and π electrons of C-C bond of ring lead to stabilization in the some part of ring as evident from intramolecular hyperconjugative interaction of σ [(C1-C2), (C1-C6), (C3-C4)] distribute to σ*[(C1-C6), (C2-C3), (C2-C10)] leading to stabilization of (~ 3e). This enhanced further conjugation with antibonding orbital of π*[(C3-C4), (C18-O19), (C1-C2), (C5-C6)] which leads to strong decalization of 17.40, 23.81, 21.99 and 18.38 KJ/mol. The NBO analysis also proved the chemical interpretation of hyperconjugation interaction and Electron Density Transfer (EDT) from filled lone electron pairs of the n(Y) of the Lewis base Y into the unfilled antibond σ*(X-H) of the "Lewis acid" X-H in X-H…..Y hydrogen bonding system [27, 28]. The intermolecular O-H….O hydrogen bonding formed by the orbital overlap between the n(O) and σ*(O-H) which result ICT cause stabilization of the H-bonded systems. The hydrogen bonding interactions leads to increase in ED of the O-H antibonding orbital. The comparison between monomer and dimer clearly demonstrate the evidence of formation of strong H-bonded interaction between oxygen (O) lone electron pair and σ*(O-H) antibonding orbitals. The magnitude of the charge transfer from lone pair of n(O19) of the hydrogen bond O atoms into the anitbonds σ*(O41-H42) to 6.59 and 17.13 KJ/mol and n (O40) to σ*(O20-H21) to 7.77 and 21.05 KJ/mol respectively as shown in Table 3 which denote the extend of intermolecular hydrogen bonding. The difference in $E^{(2)}$ energies is reasonable due to fact that the accrual of electron density in O-H bond is not only drawn from the n(O) of hydrogen – acceptor but also from the whole system.

Table 3. Second Order Perturbation Theory Analysis of Fock Matrix in NBO basis for 2,5DMBA by B3LYP/6-31G(d,p) Method

Donor (i)	ED(i) (e)	Energy (i) (a.u)	Acceptor (j)	ED (j)(e)	Energy (j) (a.u)	E(2)[a] (Kj/mol)	E(j)-E(i)[b] (Kcal/mol)	Fij[c] (a.u)
σ(C1-C2)	1.97051	-0.68406	σ*C1-C6)	0.02010	0.57207	3.97	1.26	0.063
			σ*(C2-C3)	0.01997	0.57994	2.65	1.26	0.052
π(C1-C2)	1.62112	-0.24105	π*(C3-C4)	0.31620	0.03783	17.40	0.28	0.063
			π*(C18-O19)	0.26152	0.01113	23.81	0.25	0.071
σ(C1-C6)	1.97337	-0.68485	σ*(C1-C2)	0.02864	0.56885	4.41	1.25	0.066
			σ*(C2-C10)	0.01476	0.42771	3.28	1.11	0.054
σ(C1-C18)	1.97587	-0.66848	σ*(C2-C3)	0.01997	0.57994	2.30	1.25	0.048
			σ*(C5-C6)	0.02201	0.59694	2.34	1.27	0.049
σ(C3-C4)	1.97942	-0.69256	σ*(C2-C3)	0.01997	0.57994	2.96	1.27	0.055
			σ*(C2-C10)	0.01476	0.42771	2.89	1.12	0.051

π(C3-C4)	1.66698	-0.24660	π*(C1-C2)	0.38592	0.03880	21.99	0.29	0.072
			π*(C5-C6)	0.31149	0.04423	18.38	0.29	0.066
σ(C5-C6)	1.97553	-0.69142	σ*(C1-C6)	0.02010	0.57207	3.18	1.26	0.057
			σ*(C1-C18)	0.06428	0.43595	2.71	1.13	0.050
π(C5-C6)	1.64817	-0.24285	π*(C1-C2)	0.38592	0.03880	18.54	0.28	0.065
			π*(C3-C4)	0.31620	0.03783	21.06	0.28	0.069
LP(1)O19	1.97583	-0.68405	σ*(C1-O18)	0.06428	0.43595	2.77	1.12	0.050
LP(2)O19	1.84809	-0.25543	σ*(C1-O18)	0.06428	0.43595	18.20	0.69	0.102
LP(2)O19	1.84809	-0.25543	σ*(C18-O20)	0.09858	0.34875	33.25	0.60	0.128
LP(2)O20	1.82809	-0.32590	π*(C18-O19)	0.26152	0.01113	45.20	0.34	0.113
π*(C18-O19)	0.26152	0.01113	π*(C1-C2)	0.38592	0.03880	82.20	0.03	0.075

Table 4. Second Order Perturbation Energies $\epsilon^{(2)}$ (donor acceptor) for 2,5DMBA

Donor (i)	Acceptor (j)	$E^{(2)a}$(KJmol^{-1})	E(j)-E(i)^b (a.u)	F(i,j)^c (a.u)
Within unit 1				
LP(2)O19	σ*(C1-C18)	16.44	0.66	0.094
LP(2)O19	σ*(C18-O20)	18.50	0.73	0.106
LP(1)O20	σ* (C18-O19)	10.38	1.03	0.093
LP(2)O20	π*(C18-O19)	64.29	0.31	0.129
From unit 1 to unit 2				
LP(1)O19	σ*(O41-H42)	6.59	1.17	0.079
LP(2)O19	σ*(O41-H42)	17.13	0.77	0.105
From unit 2 to unit 1				
LP(1)O40	σ*(O20-H21)	7.77	1.17	0.086
LP(1)O41	σ* (O20-H21)	21.05	0.79	0.117
Within unit 2				
LP(2)O40	σ*(C24-C39)	16.26	0.67	0.095
LP(2)O40	σ*(C39-O41)	17.63	0.73	0.104
LP(1)O41	σ*(C39-O40)	10.29	1.04	0.092
LP(2)O41	π*(C39-O40)	64.34	0.31	0.129

[a]$E^{(2)}$ means energy of hyper conjugative interaction (stabilization energy)

[b]Energy difference between donor and acceptor i and j NBO orbitals.

[c]F(i,j) is the Fork matrix element between i and j NBO orbitals.

Vibrational Analysis

The FT-IR and FT-Raman spectral data have been taken from Spectral Database for Organic Compounds [29]. The FT-IR and FT-Raman spectral data and theoretical predicted wavenumber by B3LYP/6-31G(d,p) method as shown in Table 5. As seen from the Table 5 none of the predicted vibrational wavenumber has any imaginary frequency, which indicates that the optimized structure is located at the local lowest point on the Potential Energy Surface (PES).

The title molecule has 21 atoms, which undergo 57 normal modes of vibrations. The 57 normal mode of vibrations are distributed as

$$\Gamma_{vib} = 39A' + 18A''$$

The molecule agree with C_1 point group symmetry, so all the vibrations are active in both IR and Raman absorption spectra. The detailed vibrational assignment is made by comparing the recorded wavenumber with computed ones. The computed wavenumber are usually higher than the experimental wavenumber due to the combination of electron correlation effects and

deficiencies in basis sets so proper scale factor of 0.961 is recommended by A.P. Scott [30]. After scaling down the computed wavenumber the experimental data are in good agreement with computed ones.

C-H Vibrations

The heteroatomatic structure shows the presence of C-H stretching vibrations in the region 3100-3000 cm^{-1}, which is the region for the ready identification of C-H stretching vibration [31]. In 2,5DMBA there are three C-H bonds. The expected three C-H stretching vibrations corresponds to stretching modes of C3-H7, C4-H8 and C6-H9 units. In our present study the FT-IR band at 2966 cm^{-1} in FT-IR spectrum are assigned to C-H stretching vibration. The calculated wavenumber for the mode is at 3096, 3065 and 3047 cm^{-1} (mode nos. 2-4) by B3LYP/6-31G(d,p) method. This assignment is found well with related work [31].

The bands due to C-H in-plane bending vibrations are expected in the region 1300-1000 cm^{-1}[32]. The 2,5DMBA the C-H in-plane bending vibration are recorded as a very strong band at 1384, 1273, 1216 cm^{-1} in FT-IR and 1386, 1266, 1209 cm^{-1} in FT-Raman spectrum show good correlation with computed wavenumber at 1384, 1267 and 1204 cm^{-1}(mode nos. 19, 24 and 24) by B3LYP/6-31G(d,p). The C-H out of plane bending vibrations is expected in the region 1000-750 cm^{-1} as coupled vibrations. The vibrational band computed at 937 and 890 cm^{-1}(mode nos. 34 and 35) shows good correlation with observed spectral line at 914 cm^{-1} in FT-Raman and 896 cm^{-1} in FT-I spectrum.

COOH Group Vibrations

The carboxylic acid dimer is formed by strong hydrogen bonding in solid and liquid state. Vibrational analysis of the carboxylic acid is made on the basis of carbonyl and hydroxyl group. The hydroxyl stretching and bending vibration can be identified based on the breadth and strength of the band, which are dependent on the extent of hydrogen bonding [33-35]. The non-hydrogen bonded or free hydroxyl group absorbs strongly in the region 3700-3584 cm^{-1} region while the existence of intermolecular hydrogen bond formation can lower the O-H stretching wavenumber to the 3550-3200 cm^{-1}. The wavenumber computed for O20-H21 stretching vibration is at 3621cm^{-1} (mode no.1) by B3LYP/6-31G(d,p) method. This appearance of the red shift in the O-H stretching vibration is clearly due to the formation of O-H…..O hydrogen bond. The lone pair of the oxygen (electron donor) with the O-H antibonding σ* orbital leads to increase of electron population in this orbital, followed by weakening the O-H bond which is accompanied by a lowering of the O-H stretching wavenumber. The O-H in-plane bending vibrations are normally mixed with C-C-H bending and C-C stretching vibrations. The computed wavenumber at 1291 cm^{-1} (mode no.23) by B3LYP/6-31G(d,p) method.

The O-H out-of-plane bending normally occurs in the range 700-600 cm^{-1}. The position of this band depend on the strength of the hydrogen bonding and stronger the hydrogen bond, higher the wavenumber. In presence of hydrogen bonding, the characteristic band due to out-of-plane bending is obtained at 450-350 cm^{-1}[37]. The very weak band at 661 cm^{-1} in FT-Raman spectrum are assigned to O20-H21 out-of-plane bending vibration. The computed wavenumber for this mode is at 583 cm^{-1} (mode no.43) by B3LYP/6-31G(d,p) method.

The stretching vibration of carboxylic acid (COOH) is similar to C=O stretching vibration in ketones, which is expected in the region 1740-1660 cm^{-1} [33]. In our present study, the strong band at 1688 cm^{-1} in FT-IR and 1640 cm^{-1} in FT-Raman spectrum are assigned to C18=O19 stretching vibration. The B3LYP/6-31G(d,p) method predict the wavenumber at 1735 cm^{-1} (mode no.11). The difference between the recorded and computed wavenumber may be due to presence of intramolecular hydrogen bonding between methyl groups. The computed C=O in-plane and out-of-plane bending vibration are in consistence correlation with recorded spectral data are shown in Table 5.

Table 5. Vibrational wavenumbers obtained for 2,5DMBA at B3LYP/6-31G(d,p) method [harmonic frequency (cm^{-1}), IR $_{int}$($Kmmol^{-1}$), Raman Intensity (Arb Units)]

Mode nos.	[a]Experimental (cm^{-1})		Theoretical Wavenumber (cm^{-1})			Vibrational Assignment
	FT-IR	**FT-Raman**	**B3LYP scaled**	**IR ^{int}**	**Ram^{Int}**	
1		3068ms	3621	75.66	272.68	υO-H
2	2966ms		3096	2.25	52.44	υC-H
3			3065	23.45	167.92	υC-H
4			3047	10.39	70.40	υC-H
5			3012	19.74	18.81	υ_{asym} $C10H_3$
6		2991s	3006	14.28	13.78	υ_{asym} $C14H_3$
7	2925vw		3005	8.23	10.26	υ_{asym} $C10H_3$
8			2975	19.22	63.28	υ_{asym} $C14H_3$
9			2938	21.24	11.21	υ_{sym} $C10H_3$
10			2922	31.96	53.77	υ_{sym} $C14H_3$
11	1688s	1640ms	1735	299.94	9.75	υ C18=O19
12	1613m	1616ms	1605	2.30	142.22	υ C-C
13	1571ms	1573s	1555	24.00	8.18	υ C-C
14	1503ms		1482	23.33	14.78	υ C-C + β C-H
15			1454	12.52	61.75	$C14H_3$ asym.deform
16	1467ms	1442ms	1441	5.41	6.26	$C14H_3$ asym.deform
17			1435	9.07	2.16	$C10H_3$ asym.deform

Table 5. Cond.) Vibrational wavenumbers obtained for 2,5DMBA at B3LYP/6-31G(d,p) method [harmonic frequency (cm^{-1}), IR $_{int}$($Kmmol^{-1}$) Raman Intensity (Arb Units)]

Mode nos.	[a]Experimental (cm^{-1})		Theoretical Wavenumber (cm^{-1})			Vibrational Assignment
	FT-IR	FT-Raman	**B3LYP scaled**	**IR ^{int}**	**Ram^{Int}**	
18	1414ms		1431	4.66	81.06	$C10H_3$ asym.deform
19	1384s	1386s	1384	3.65	69.54	β C-H
20	1377ms		1377	2.62	1.33	ρ$C10H_3$
21	1367ms		1375	0.17	13.00	ρ$C14H_3$
22	1311m		1332	107.40	35.03	υ C18-C28 + β O20-H21
23		1306s	1291	10.16	4.52	υ C-C + β O20-H21
24	1273m	1266s	1267	4.89	5.80	β C-H
25	1216vs	1209ms	1204	13.99	21.95	β C-H + β O20-H21
26			1184	6.96	2.38	υ C-C + β C-H
27	1161vs	1163w	1146	156.29	0.20	υ C-C + β C-H
28	1086vs		1138	134.00	15.25	υ C-C + β C-H
29	1037vs		1043	89.13	17.51	υ C1-C18 + υ C18-O20 + β C-H
30			1029	7.28	10.68	ρ $C10H_3$
31			1022	1.11	76.94	ρ $C14H_3$

32	922ms		998	1.30	57.63	β C- C10H_3
33			976	4.55	6.10	β C- C10H_3
34		914w	937	0.16	12.07	β C- OH
35	896m		890	1.10	43.14	β C- OH
36			890	0.05	81.06	β C-C-C

Table 5. (Cond.). Vibrational wavenumbers obtained for 2,5DMBA at B3LYP/6-31G(d,p) method [harmonic frequency (cm^{-1}), IR $_{int}$($Kmmol^{-1}$) Raman Intensity (Arb Units)]

Mode nos.	[a]Experimental (cm^{-1})		Theoretical Wavenumber (cm^{-1})			Vibrational assignment
	FT-IR	FT-Raman	B3LYP scaled	IR ^{int}	Ram^{Int}	
37	821m		808	7.40	97.25	γ C-C-C + γ O20-H21
38	783ms	765vs	756	33.06	47.53	γ C1-O18 + γ C-C-C
39	771ms	743w	736	1.58	5.73	β C-C-C
40	747s		702	11.87	5.41	β C-C-C + υ C1-C18
41	682ms	679w	684	14.54	39.43	γ C-C-C + γ O20-H21
42	676ms		636	47.75	45.63	β C18=O19 + β O20-H21
43	661s		583	91.95	9.37	β O20-H21
44	512ms		502	0.86	8.79	γ C-C-C + γ O20-H21
45	505s	481vs	500	9.13	89.07	β C-C-C + β O20-H21
46			457	1.14	77.76	υ C3-C14
47		419m	417	5.97	90.11	γ C-C-C
48			381	1.20	100.00	β C2-C10H_3 + β C18=O19
49			361	1.94	76.48	γ C2-C1OH3 + γ C5-C14H_3
50		326m	306	0.14	48.33	γ C2-C1OH_3 + γ C5-C14H_3
51		245vw	296	2.72	32.96	β C2-C1OH_3 + β C5-C14H_3
52		190s	196	0.21	29.00	β C5-C14H_3 + β COOH
53			184	0.22	30.73	t C1OH_3
54		160m	154	1.43	60.99	γ C-C-C
55			118	0.23	25.83	γ C2-C1OH_3 + γ C5-C14H_3
56			38	0.95	37.64	tC1-COOH
57			31	0.02	97.25	τ C14H_3

IR $_{int}$ - IR intensity; $Kmmol^{-1}$ Ram^{Int} –Raman Intensity; w-weak; vw- very weak; s-strong; vs-very strong; m-medium; br, sh- broad, shoulder, υ - stretching; υ_{sym} – symmetric stretching ; υ_{asy}- asymmetric stretching ; β- in plane bending ; γ- out-of –plane bending ; ω – wagging ; t- twisting ; δ –scissoring ; τ- torsion.

[a]Taken from Ref.[29].

Ring Vibrations

In 2,5DMBA there are six equivalent C-C bonds in the ring and one more C-C bond is outside of the ring system so we expect seven C-C stretching vibrations. In addition to that there are several C-C-C in-plane and C-C-C out-of-plane bending vibration modes of the ring carbons. Due to high symmetry of the benzene ring, many modes of vibrations are infrared inactive. In general, the bands of variable intensity and are observed at 1625-1590, 1590-1575, 1540-1470, 1465-1430 and 1380 -1280 cm^{-1} from the wavenumber ranges given by Varsanyi [31] for the five bands in the region. In 2,5DMBA the wavenumber computed by B3LYP/6-31G(d,p) method at 1605, 1555, 1482, 1291, 1184, 1146, 1136 cm^{-1}(mode nos. 12, 13, 14, 23, 26, 27, 287) shows good complement with recorded spectral data at 1613, 1571, 1503, 1616, 1086 cm^{-1} in FT-IR and 1616, 1573, 1306, 1163 cm^{-1} in FT-Raman spectrum are assigned to C-C stretching mode of the 2,5DMBA

molecule. The in-plane deformation vibrations at higher wavenumber than the out-of-plane vibration. Shimanouchi et al. [38] gave the wavenumber date for these vibrations for five different benzene derivatives as results of normal coordinate analysis. The in-plane and out-of-plane bending vibrations are in consistence correlation with recorded spectral data.

Methyl Group Vibrations

The title molecule 2,5DMBA under consideration possesses two CH_3 group in second and fifth position. In aromatic compounds, the CH_3 asymmetric stretching vibrations are expected in the range 2925-3000 cm^{-1} and symmetric CH_3 vibrations in the range 2905-2940 cm^{-1}[39, 40]. The asymmetric stretching modes of the methyl group are calculated at 3012, 3006, 3005 and 2975 cm^{-1}(mode nos.5, 6, 7 and 8) by B3LYP/6-31G(d,p) method show good agreement with recorded FT-IR spectrum at 2966, 2925 cm^{-1} and 2991 cm^{-1} in FT-Raman spectrum respectively. The computed wave number for symmetric mode by B3LYP/6-311G(d,p) method is at 2938 and 2922 cm^{-1} .The recorded FT-IR and FT-Raman spectrum does not show any such a kind of vibrational band in this region, this may be due to methyl group attached to the aromatic ring are usually down shifted due to electronic effects [41].

The asymmetric deformations are expected in the region 1400-1485 cm^{-1} [42]. The medium strong bands in FT-IR at 1467 cm^{-1} and 1442 cm^{-1} in FT-Raman spectra are assigned to CH_3 asymmetric deformation, the computed wavenumber exactly correlate with experimental value at 1441 cm^{-1} as shown in Table 5. In many methyl substituted molecules, the symmetric deformation of CH_3 is expected to appear in the range 1360-1390 cm^{-1}[40] with an intensity varying from medium to strong. The computed wavenumber at 1377 cm^{-1}(mode no. 20) is assigned to CH_3 symmetric deformation for 2,5DMBA, the recorded FT-IR spectrum medium band at 1377 and 1367 cm^{-1} respectively are assigned to CH_3 symmetric deformation.

HOMO LUMO Analysis

Both Highest Occupied Molecular Orbital (HOMO) and Lowest Unoccupied Molecular Orbital (LUMO) are major orbital which is responsible for chemical reaction. The HOMO energy denote the ability of give electrons and LUMO denote the ability to accept the electrons, the gap between HOMO and LUMO characteristic the molecular chemical stability [43].

The surface of frontier molecular orbital were described to understanding the bonding scheme of 2,5DMBA molecule i.e HOMO-1, HOMO, LUMO and LUMO +1 four important molecule orbital were examined iThe predicted frontier molecular orbital for 2,5DMBA is shown in Figure 5. The HOMO is located over methyl and COOH group, the HOMO→LUMO transitions denote the electron density will transfer from methyl and COOH to the ring systems. The energy gap between HOMO and LUMO is 0.195 eV. The energy gap between HOMO and LUMO has been proving that bioactivity from intramolecular charge transfer [44].

Molecular Electrostatic Potential (MEP) Analysis

The 3D plot of Molecular Electrostatic Potential (MEP) for 2,5DMBA is shown in Figure 6. The MEP is a plot of electrostatic potential mapped onto the constant electron density surface. In majority of MEP diagram the electrophilic attack indicate as red colour and nucleophilic attack indicate blue colour. The MEP diagram also shows the molecular size, shape, as well as negative, positive and neutral electrostatic potential by colour grading and it plays a vital role for researcher for analysing the physicochemical property [45]. The different values of electrostatic potential at the surface of the 2,5DMBA molecule is presented in different colour. Electrostatic potential is increased in the order of red<orange<yellow<green<blue. The colour code of the maps are found in the range -0.068 a.u (deepest red) to 0.0399 (deepest blue). Where red indicate strongest repulsion and blue indicate strong interaction. As seen from the Figure 6. The negative potential present over COOH and CH_3 group positive potential region over ring systems and hydrogen atoms. The predominance of the light green represents the potential halfway between the two extreme red and dark blue colour, provides the information about the region where the compound can be intermolecular interaction.

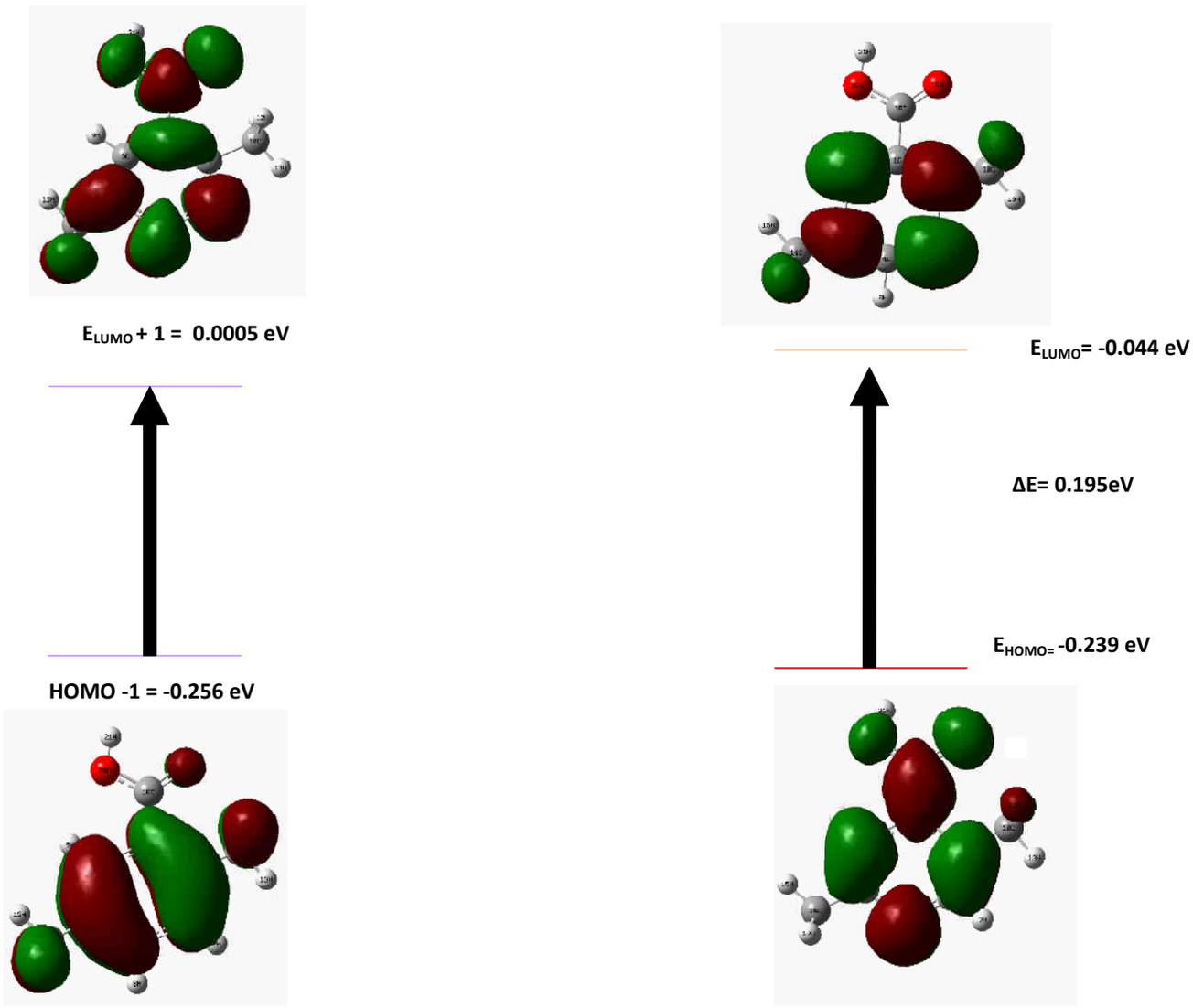

Fig. 5 The atomic orbital compositions of the frontier molecular orbital for 2,5DMBA

CONCLUSION

By the use of quantum mechanical approach we thoroughly analyzed the conformational stability, molecular geometry, vibrational spectra, HOMO and LUMO energy for 2,5DMBA molecule. Based on the calculated energies of different conformer we conclude that C2 is the most stable conformer when compared to others. The optimized geometry for 2,5DMBA is in good agreement with available related experimental crystal data. The difference between the observed and scaled wavenumber values of most of the fundamentals are very small. The NBO analysis reproduces the presence of strong hydrogen bonding, intermolecular delocalization and hyper conjugation in the 2,5DMBA molecule. The lowering of the HOMO-LUMO energy gap value shows the substantial influence on the intermolecular charge transfer and bioactivity of the molecule.

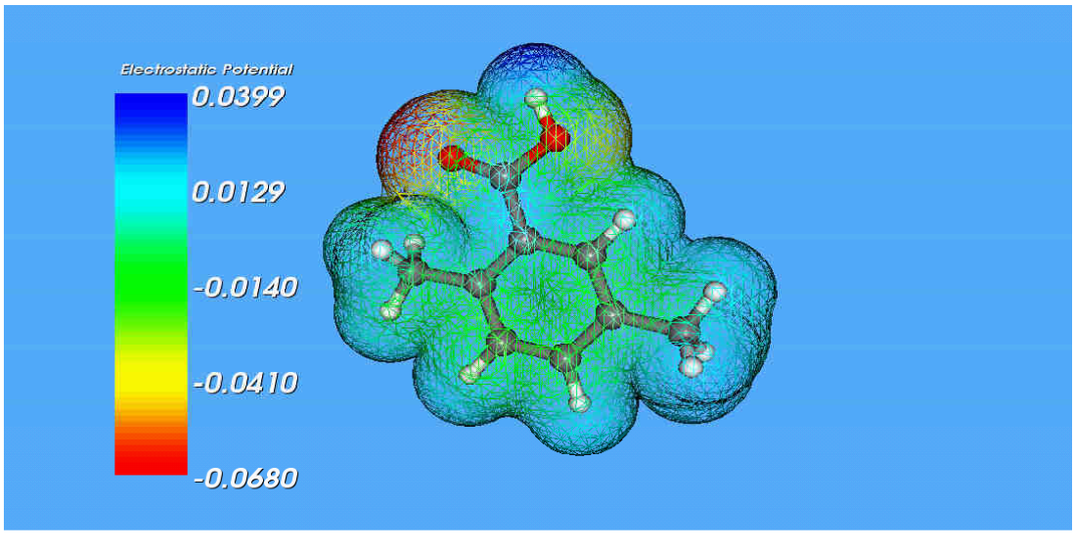

Fig.6 Molecular Electrostatic Potential Diagram of 2,5DMBA

ACKNOWLEDGEMENTS

The authors of this manuscripts are very much thankful to Database for Organic Compounds (SDBS) for providing FT-IR and FT-Raman spectrum.

The authors are also thankful to Quantum Computational Research Lab facility provided by the administration of St Joseph's College of Arts & Science (Autonomous), Cuddalore for computational works.

REFERENCE

1. O.D.Tyagi, M.Yadav, Textbook of Synthetic Drugs, Fifth Edn. Anmol Publications, New Delhi, 1990, p.49.
2. M.Karabacak, S.Bilgili, A.Atac, Spectrochimica. Acta. 134A (2015) 598-607.
3. M.Karabacak, L.Sinha, O. Prasad, A.M. Asiri, M. Cinar, V. K. Shukla Spectrochimica Acta 123A (2014) 352-362.
4. N.Balamurugan, C.Charanya, S.SampathKrishnan, S. Muthu, Spectrochimica.Acta. 137A (2015) 1374-1386.
5. V. Krishnakumar, R. Mathammal, S. Muthunatesan, Spectrochimica Acta. 70A (2008) 201-209
6. D. Sajan, J. Binoy, B. Pradeep, K. Venkatakrishnan, V.B. Kartha, I.H. Joe, V.S. Jayakumar, Spectrochim. Acta. 60A (2004) 173-180.
7. J.P. Abraham, I.H. Joe, V. George, O.F. Nielson, V.S. Jayakumar, Spectrochim. Acta. 59 A (2003) 193-199.
8. J.Binoy, J.P.Abraham, I.H.Joe, V.S.Jayakumar, J.Aubard, O.F.Nielson J.Raman Spectrosc. 36 (2005) 63-72.
9. M.J. Frisch, G.W. Trucks, H.B. Schlegel, G.E. Scuseria,M.A. Robb, J.R. Cheeseman, G. Scalmani, V. Barone, B. Mennucci, G.A. Petersson, H. Nakatsuji, M. Caricato, X. Li, H.P. Hratchian, A.F. Izmaylov, J. Bloino, G. Zheng, J.L. Sonnenberg, M. Hada, M. Ehara, K. Toyota, R. Fukuda, J. Hasegawa, M. Ishida, T. Nakajima, Y.Honda, O. Kitao, H. Nakai, T. Vreven, J.A. Montgomery Jr., J.E. Peralta, F. Ogliaro, M. Bearpark, J.J. Heyd, E. Brothers, K.N. Kudin, V.N. Staroverov, R. Kobayashi, J. Normand, K. Raghavachari, A. Rendell, J.C. Burant, S.S. Iyengar, J. Tomasi, M. Cossi, N. Rega, J. M. Millam, M. Klene, J.E. Knox, J.B. Cross, V. Bakken, C. Adamo, J. Jaramillo, R. Gomperts, R.E. Stratmann, O. Yazyev, A.J. Austin, R. Cammi, C. Pomelli, J.W. Ochterski, R.L. Martin, K. Morokuma, V.G. Zakrzewski, G.A. Voth, P. Salvador, J.J. Dannenberg, S. Dapprich, A.D. Daniels, O. Farkas, J.B. Foresman, J.V. Ortiz, J. Cioslowski, D.J. Fox, Gaussian-09, Revision A.02, Gaussian, Inc., Wallingford CT, 2009.
10. H.B. Schlegel, J. Comput. Chem. 3 (1982) 214-218.
11. A. Frisch, A.B. Nielson, A.J. Holder, GAUSSVIEW User Manual, Gaussian Inc, Pittsburgh, PA, (2000).
12. G. Keresztury, S. Holly, J. Varga, G. Besenyei, A.Y Wang , J. R. Durig, Spectrochim. Acta 49A (1993) 2007-2017.

13. G .Keresztury, J. M .Chalmers, and P. R. Griffith (Eds.), Raman Spectroscopy: Theory, in Hand book of Vibrational Spectroscopy, Vol 1, John Wiley &Sons Ltd., New York, 2002.
14. F.H.Allen, Acta. Crystallogr. 58B (2002) 380-386.
15. P.B.Nagabalasubramanian, S.Periyandy, S.Mohan, Spectrochim. Acta. 73A (2009) 277 – 280.
16. T.Karthick, V.Balachandran, S.Perumal, A.Nataraj, J.Mol.Struct. 1005(2011) 192-201.
17. V.Balachandran, S.Rajeswari, S.Lalitha, J.Mol. Struct. 1007(2012) 63-73.
18. G.A. Jaffrey, An Introduction to Hydrogen Bonding, Oxford University Press, 1997
19. V.Krishnakumar, V.Balachandran, T.Chithambarathanu, Spectrochim.Acta.62A (2005) 918-925.
20. L.J.Pejov, M.Trpkovska, B.S.Optrajanov, Spectrosc.Lett.32 (1999) 361-369.
21. I.G.Binve, Y.I.Binev, J.Mol.Struct.435(1997) 235-245.
22. P.Politzer, D.G.Truhlar (Edn). Chemical Applications of Atoms and Molecular Electrostatic Potential, Plessum Press, Ny, 1981.
23. S.Subash chandrabose, A.R.Krishnana, H.Saleem, R.Paramashwari, N.Sundaraganesan, V.Thanikachalam, G.Maikandan, Spectrochim. Acta. 77A (2010) 877-884.
24. C.James, A.Amal raj, R.Reghunathan, I.H.Joe, V.S.Jayakumar, J.Raman.Spectrosoc. 37 (2006) 1381-1392.
25. J.N.Liu, Z.R.Chen, S.F.Yuan, J.Zhejiang, Univ.Sci. 6B (2005) 584-589.
26. M. Szafran, A.Kamosa, E.B.Adamska, J.Mol. Struct. (THEOCHEM) 827(2007) 101- 107.
27. A.E.Reed, L.A Curtiss, F.Weinhold, Intermolecular interactions from a natural bond orbital, donor-acceptor view point, Chem.Rev. 88(1988) 899-926.
28. J.P.Foster, Weinhold, Natural orbitals, J.Am.chem. Soc. 102(1980) 7211-7218.
29. SDBS Web : http://sdbs.db.aist.go.jp (National Institute of Advanced Industrial Science and Technology, 01.10.2015)
30. A.P.Scott, L.Radom, J.Phys.Chem.100(1996) 16502-16513.
31. G.Varsany, Vibrational Spectra of Benzene Derivatives, Academic Pess, New York, 1969.
32. K.C.Modhi, R.Baraman, M.K.Sharma, Ind.J.Phys. 68B (1994) 189-195.
33. D.L.Vein, N.B.Colthup, W.G.Fatley, J.G.Grasselli, The Handbook of Infrared and Raman Characteristic Frequencies of Organic Molecules, Academic press, New York, 1991.
34. N.B.Colthup, L.H.Daly, S.E.Wiberly, Introduction to Infrared and Raman Spectroscopy, Academic press, Newyork, 1990.
35. G.Socretes, Infrared and Raman characteristic Group Frequeices: Tables and Charts, third edn. Wiley, Chichester, 2001.
36. C.Castigloni, M.Delzoppo, P.Zulliani, G.Zerbi, Syn.Metal. 74 (1995) 171-174.
37. L.J.Bellamy, The Infrared Spectra of Complex Molecules, Wiley , New York, 1959.
38. T.Shimanouchi, Y.kakiuti, I.Gam, J.Chem.Phys. 25(1956) 1245-1251.
39. N.B.Colthup, L.H.Daly, S.E.Wiberly, Introduction of Infrared and Raman Spectroscopy, 3rd edn, Academic Pres, New York, 1990.
40. N.P.Roeges, A Guide to the Complete Interpretation of Infrared Spectra of Organic Structures, Wiley, New York, 1994.
41. W.O.George, S.Mcintyre, Introduction to Spectroscopy, John Wiley, New York, 1987
42. N.P.Roeges, A Guide to the Complete Interpretation of Infrared Spectra of Organic Structures, Wiley, New York, 1994.
43. Y.Ataly, D.Avci, A.BaŞoğlu, Struct Chem, 19 (2008) 239
44. C.Ravikumar, I.H.Joe, V.S.Jayakumar, Chem. Phys.Lett. 460 (2008) 552-558.
45. J.S.Murry, K.Sen, Molecular Electrostatic Potential Concepts and Applications, Elsevier, Amsterdam, 1996.